OBSERVATIONS OF A SYNCHRONOUS SATELLITE WITH THE HAYSTACK RADAR

Grodon L. Guernsey, et al

Massachusetts Institute of Technology

Prepared for:

Air Force Systems Command

13 December 1972

UNCLASSIFIED

Security Classification

DOCUMENT CONTROL DATA – R&D

(Security classification of title, body of abstract and indexing annotation must be entered when the overall report is classified)

1. ORIGINATING ACTIVITY *(Corporate author)* Lincoln Laboratory, M.I.T.	2a. REPORT SECURITY CLASSIFICATION Unclassified 2b. GROUP None

3. REPORT TITLE

Observations of a Synchronous Satellite with the Haystack Radar

4. DESCRIPTIVE NOTES *(Type of report and inclusive dates)*

Technical Note

5. AUTHOR(S) *(Last name, first name, initial)*

Guernsey, Gordon L. and Slade, Chaloner B.

6. REPORT DATE	7a. TOTAL NO. OF PAGES	7b. NO. OF REFS
13 December 1972	32	2

8a. CONTRACT OR GRANT NO. F19628-73-C-0002 b. PROJECT NO. 1228 c. Element No. 33601r d.	9a. ORIGINATOR'S REPORT NUMBER(S) Technical Note 1972-41 9b. OTHER REPORT NO(S) *(Any other numbers that may be assigned this report)* ESD-TR-72-351

10. AVAILABILITY/LIMITATION NOTICES

Approved for public release; distribution unlimited.

11. SUPPLEMENTARY NOTES	12. SPONSORING MILITARY ACTIVITY
None	Air Force Systems Command, USAF

13. ABSTRACT

The Haystack planetary radar has been used to observe the Lincoln Experimental Satellite (LES-6). The principal characteristics of the radar signature derived from these observations are related to the physical features of the satellite.

14. KEY WORDS

satellite observations Haystack radar LES-6

I

UNCLASSIFIED

Security Classification

MASSACHUSETTS INSTITUTE OF TECHNOLOGY

LINCOLN LABORATORY

OBSERVATIONS OF A SYNCHRONOUS SATELLITE WITH THE HAYSTACK RADAR

G. L. GUERNSEY
C. B. SLADE

Group 96

TECHNICAL NOTE 1972-41

13 DECEMBER 1972

LEXINGTON MASSACHUSETTS

The work reported in this document was performed at Lincoln Laboratory, a center for research operated by Massachusetts Institute of Technology, with the support of the Department of the Air Force under Contract F19628-73-C-0002.

ABSTRACT

The Haystack planetary radar has been used to observe the Lincoln Experimental Satellite (LES-6). The principal characteristics of the radar signature derived from these observations are related to the physical features of the satellite.

Accepted for the Air Force
Joseph J. Whelan, USAF
Acting Chief, Lincoln Laboratory Liaison Office

OBSERVATIONS OF A SYNCHRONOUS SATELLITE WITH THE HAYSTACK RADAR

A ground station for space communications, radar, and radio astronomy research was completed at Tyngsboro, Massachusetts, in 1964.[1] This installation, which is named Haystack, employs a 120-foot-diameter fully steerable antenna enclosed in a metal space-frame radome (Figure 1). Advanced design and construction techniques were developed to achieve a reflector with a very precise parabolic contour. The antenna operates very efficiently at wavelengths of 3 cm and also provides a useful capability at wavelengths as short as 8 mm. A "plug-in" equipment room behind the reflector makes it possible to utilize the antenna for a variety of active and passive experiments. To provide appropriate control for the very narrow antenna beam, a general-purpose digital computer has been integrated into the facility. The RF configuration of the antenna is compatible with the use of high-power transmitters and cooled, low-noise equipment. A versatile 1-Mw average power, high-voltage supply has been provided for energizing transmitting equipment. This installation provides a unique capability in the microwave portion of the spectrum for communications, radar, and radio astronomy.

Haystack was established by Lincoln Laboratory with support from the Electronic Systems Division of the United States Air Force. It is now operated by MIT for a consortium of Universities known at the North East Radio Observatory Corporation (NEROC).

During the summer of 1971, Mr. Robert J. Bergemann, Jr. and Dr. Gordon L. Guernsey of Lincoln Laboratory suggested that the Haystack radar be used to observe the small, synchronous satellite LES-6.[2] On 1 September 1971, a team consisting of Mr. Richard P. Ingalls and Dr. Stanley H. Zisk of NEROC and the two Lincoln staff, detected the radar echo from LES-6. A second detection was made on 15 September 1971 and extensive data were recorded.

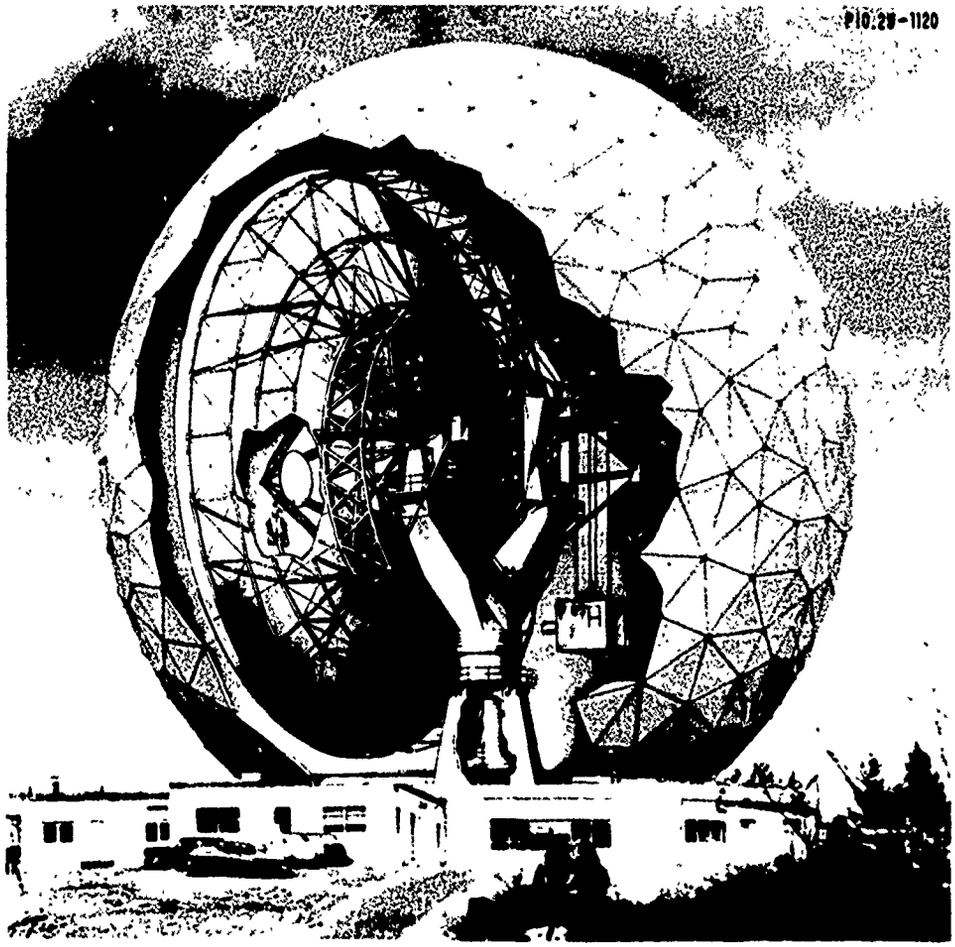

Fig. 1. Haystack planetary radar.

A brief description of the Haystack radar and its applicability to satellite observations is presented first. An attempt to relate the radar measurements to the known properties of LES-6 follows.

THE HAYSTACK RADAR

The Haystack radar, originally designed for planetary observations, was not reconfigured for these satellite measurements. The radar frequency is 7840 MHz, for which the antenna gain is 66 dB. During the measurements, the transmitter was operated so that it radiated 100 kilowatts (it is capable of 300 kilowatts CW). Under favorable atmospheric conditions, the system noise temperature is 75^{o}K. The maximum pulse length for a target at synchronous altitude distance is about 0.2 seconds. With this pulse length, the single-pulse signal-to-noise ratio on a 1-square-meter target at synchronous altitude (approximately 40,000 kilometers slant range) is calculated to be + 19 dB. The radar radiates right circular polarization and the RF plumbing permits receiving the matched polarization (left circular), or the orthogonal polarization (right circular). Only one receiver channel is presently available, but it can be switched between the two polarizations on alternate pulses.

On 15 September 1971, the sixth Lincoln experimental satellite (LES-6) was observed by the radar. This satellite is shown in Figure 2. Using pulses of 0.2048 seconds duration repeated at intervals of 0.470 seconds radar echoes were obtained that varied with time as shown in Figure 3, a typical data segment.

The radar is coherent and the receiver output is quadrature video. The two output voltages were sampled with an 8-bit A-to-D converter, 128 times for each pulse at intervals of 1.6 milliseconds. A Fourier transform was computed in real time and thus a complete Doppler spectrum was computed at intervals of 0.470 seconds. Thus, in effect there are 128 contiguous receiver channels each matched in bandwidth to the transmitted pulse (4.88 Hz per channel). Figure 4 shows a typical Doppler spectrum computed from the average of 108 successive spectra produced as described above.

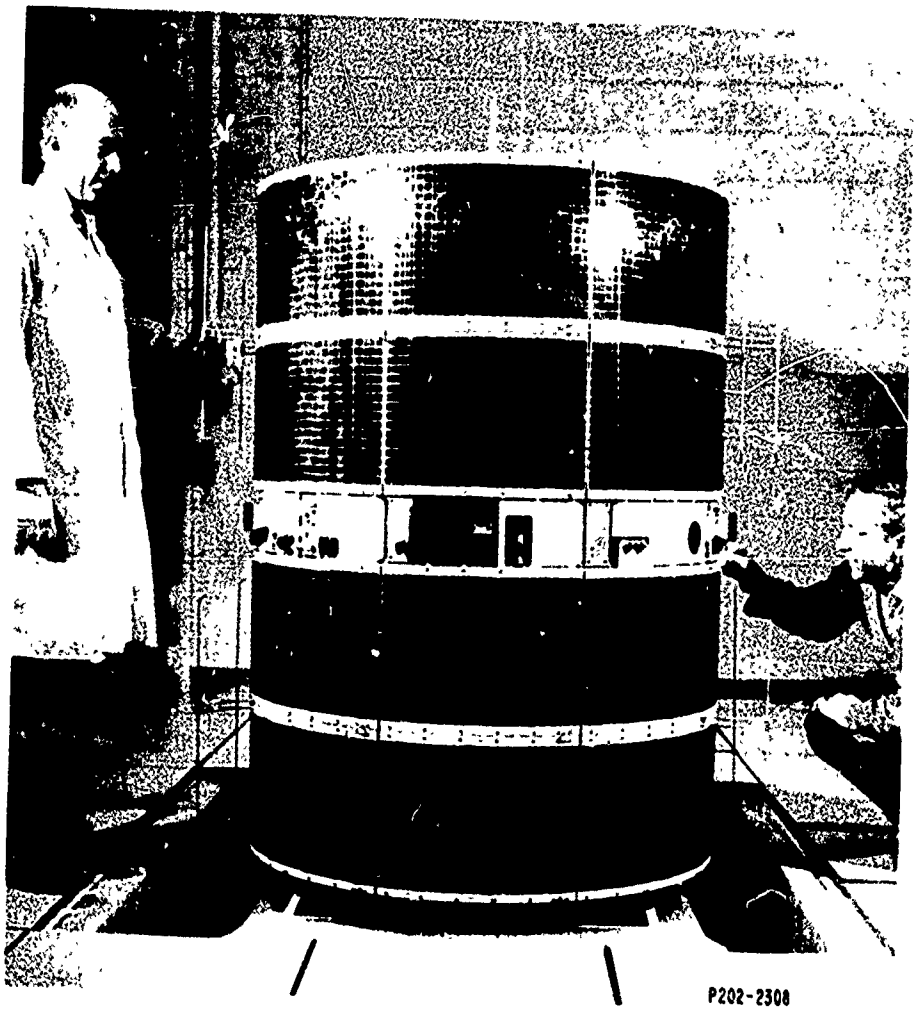

Fig. 2. The satellite LES-6.

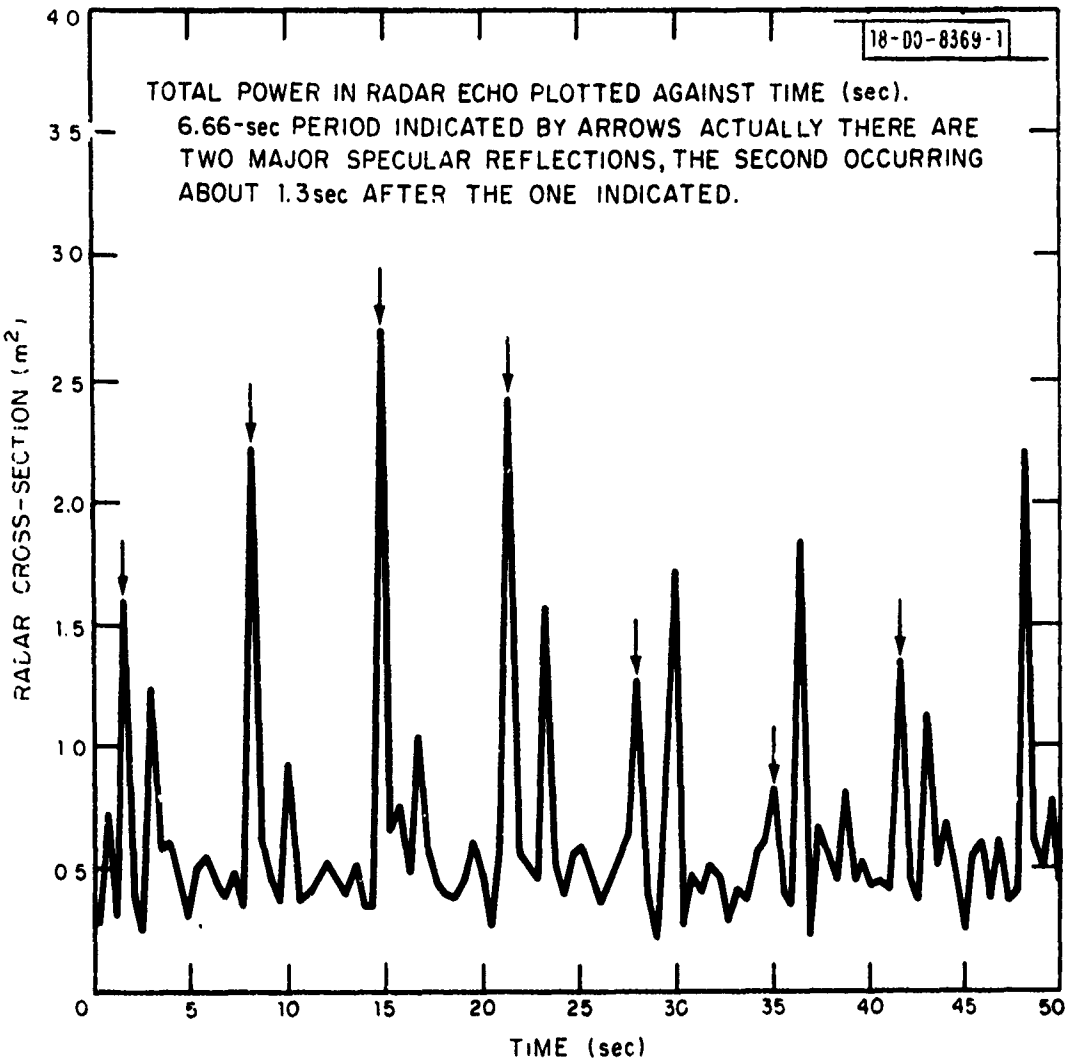

Fig. 3. Haystack observations of LES-6, 15 September 1971.

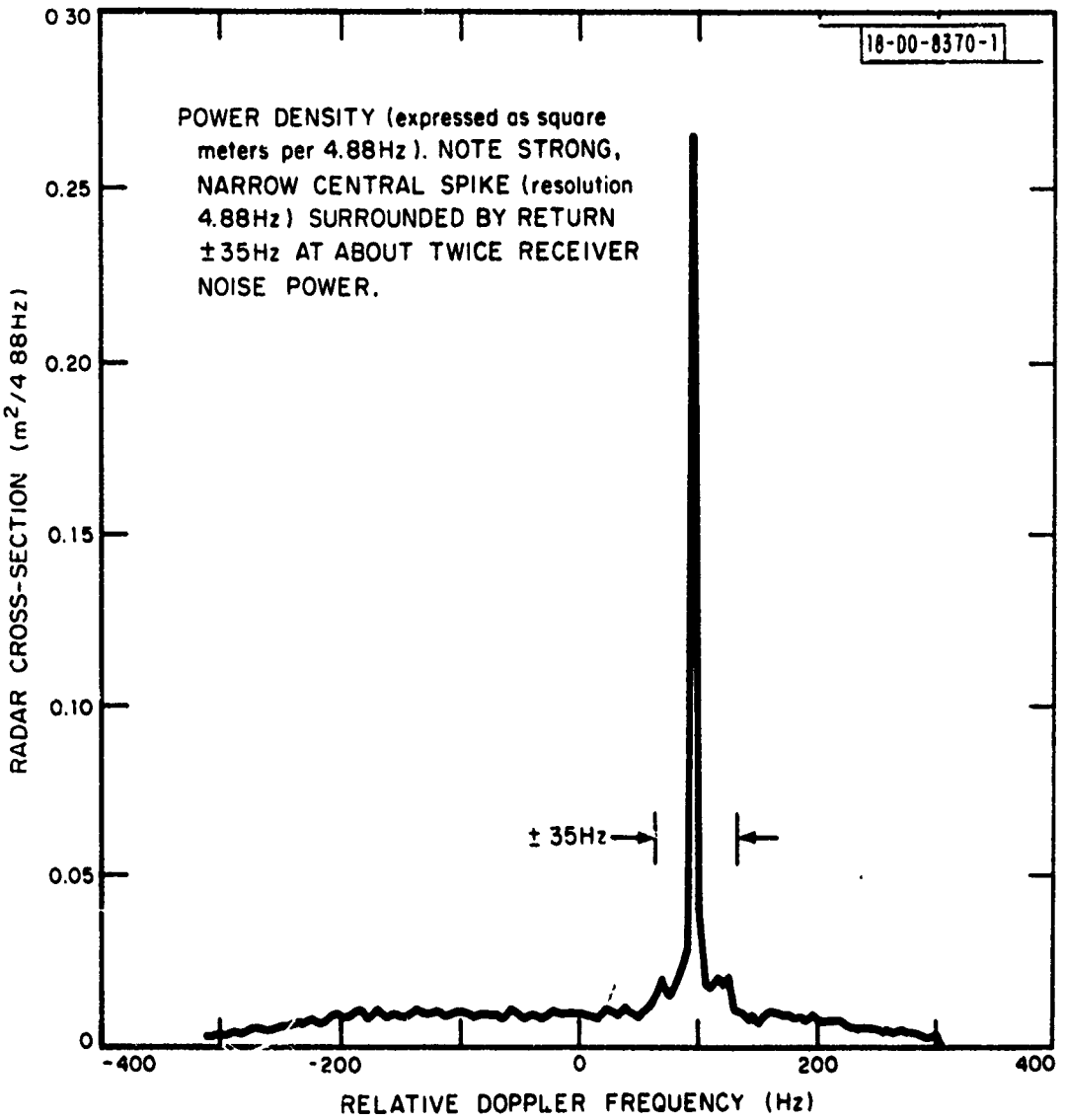

Fig. 4. Haystack observations of LES-6, 15 September 1971.

ANALYSIS OF THE OBSERVATIONS

We will now try to relate the known characteristics of the satellite to the principal observed features of the radar echoes.

Figure 5 shows the principal features of LES-6. The body of the satellite is a right circular cylinder 168 cm long and 122 cm in diameter. Most of the cylindrical surface is covered with solar cells. The continuity of the surface is broken by two circular arrays of VHF dipoles. Moreover, each dipole is backed by a slot radiator arranged to provide circular polarization.

Titan III-C No. 5 placed LES-6 into a 2.9° inclined synchronous orbit on 26 September 1968. On-board thrusters keep it on station at 38°W longitude. Nominally, the satellite is spinning about its axis of symmetry at about 10 rpm and the axis is parallel to the earth's axis (actually there is a 2.2° misalignment of the spin axis from the body axis). The dipole-plus-slot antennas are electrically switched so as to direct a beam toward the earth (hence the terminology "electrically despun").

The Haystack radar is located at 43°N latitude and 70°W longitude. The position of the satellite relative to the radar is shown in Figure 6. Since the spin axis of the satellite is within a few degrees of normal to its orbital plane and its orbital plane has about a one degree inclination, the spin axis is within a few degrees of parallel to the earth's polar axis and at 43°N latitude the mean aspect angle is about 6.6°. During an orbital period (one sidereal day) this will vary $\pm 3^{\circ}$ because of the inclination of the orbit and the tilt of the spin axis from the orbital plane. In addition, it will vary $\pm 2.2^{\circ}$ because of the wobble of the satellite (non-coincidence of the spin axis and the cylinder axis) with a period of 6.6 seconds.

The position of the satellite, at the times of observation, in azimuth and elevation from the radar is plotted in Figure 7, as is a computed position from Lexington for 19 days earlier, simply to indicate the phase of the satellite in its orbit during observation. The satellite was evidently in the quadrant of its orbit between the descending node and the maximum southern latitude. This is consistent with the mean Doppler frequency observed by the radar which is plotted in Figure 8. Mean Doppler

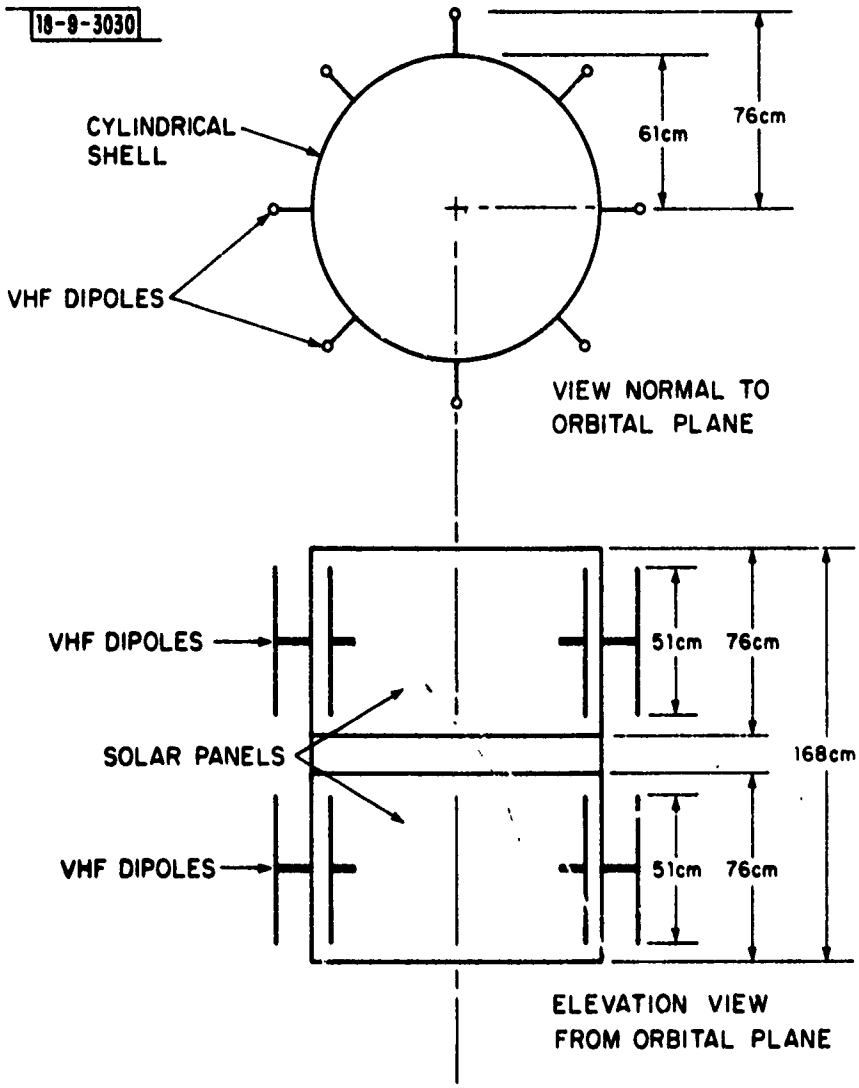

Fig. 5. LES-6 external dimensions.

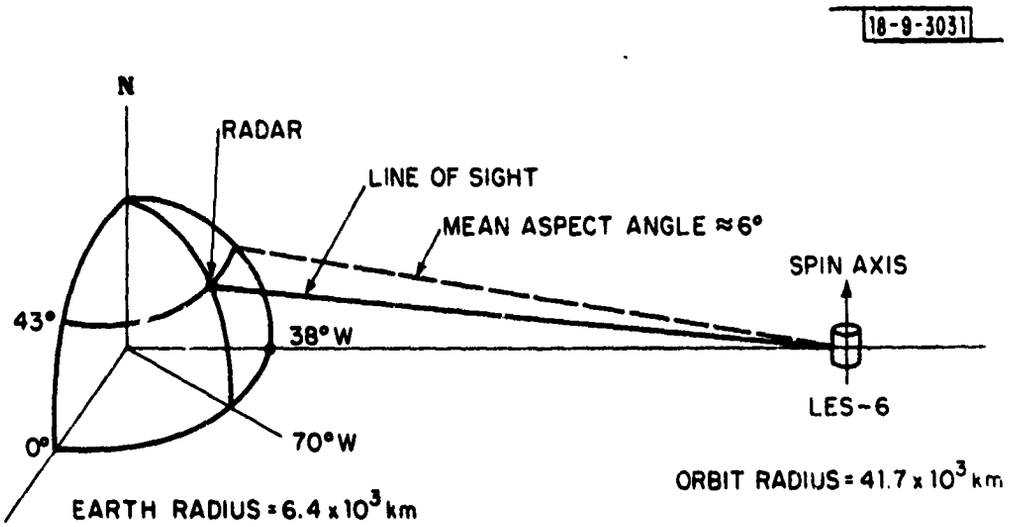

Fig. 6. Relative position of LES-6 and Haystack.

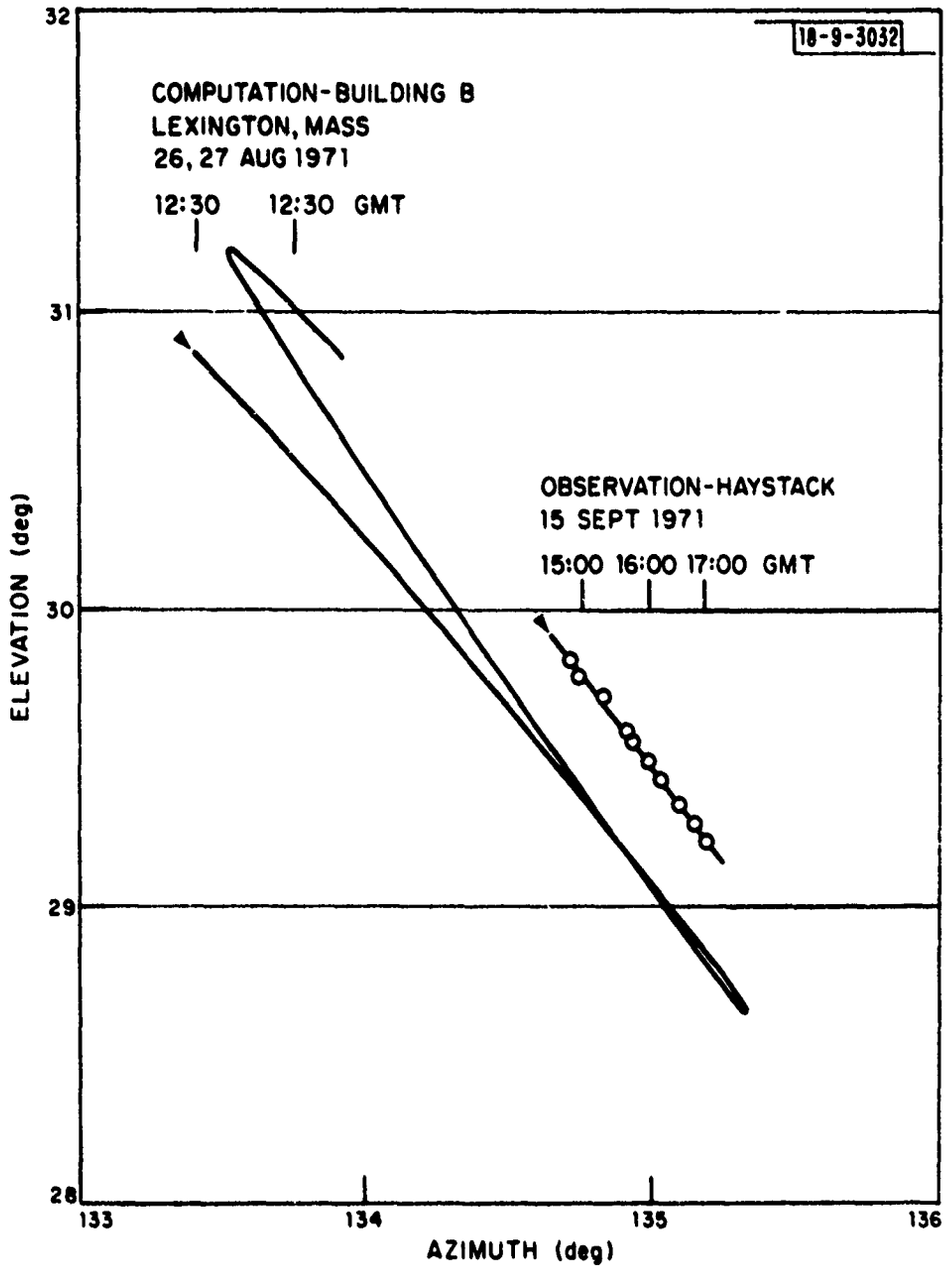

Fig. 7. Azimuth and elevation of LES-6.

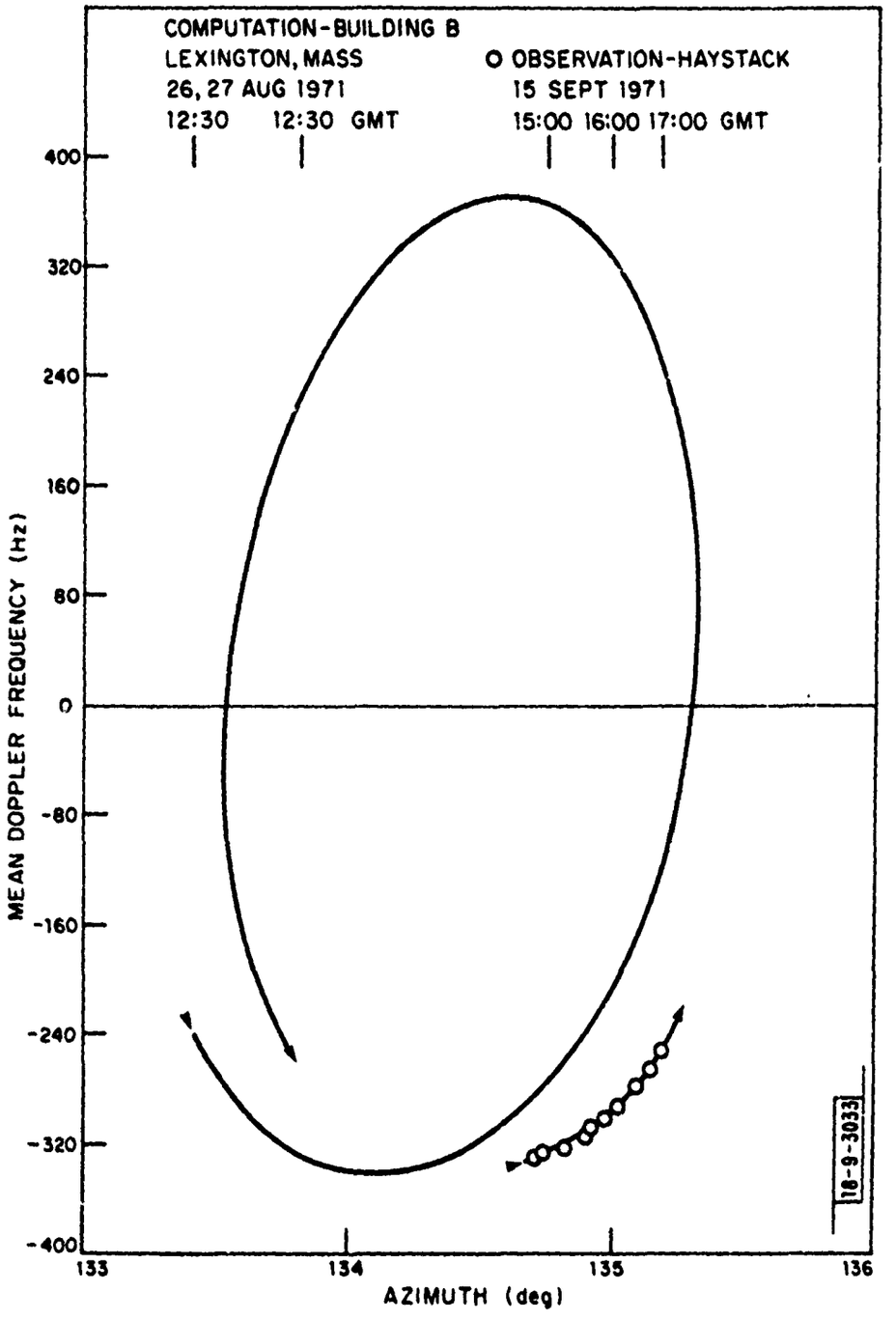

Fig. 8. Mean Doppler frequency of LES-6.

frequency is negative and decreases in absolute value with time over the period of a little more than two hours. Thus the satellite is receding at a decreasing rate. Again a comparison is made with the Doppler computed* for a complete orbit which shows that the maximum receding Doppler occurs at about the descending node and the maximum approaching Doppler occurs at about the ascending node. The skewing of the position and Doppler patterns (Figures 7 and 8) is occasioned by the radar and satellite being at different longitudes. The lack of closure in the computed values can be the result of a combination of three factors:

- the satellite does drift in longitude,
- there are residual errors in the orbital data, and
- there are approximations in the computer program employed.

The radar echoes of Haystack from LES-6 were processed by a fast Fourier transform producing a Doppler spectrum for each pulse. About 128 of these spectra (0.2048-sec pulses with a 0.470-sec repetition period for 60 seconds) were then averaged to produce the sort of Doppler spectrum illustrated in Figure 9. Figure 9 shows the signal $(S_i)^\dagger$ and noise $(N_i)^\dagger$ on a relative linear power scale in 100 (out of 128) contiguous digital Doppler filters of width 4.88 Hz. This spectrum obtains for the observation at 15:38:30 GMT but is representative of the information available from similar observations. The noise power per Doppler bin is essentially constant with Doppler frequency, as expected, at a relative value of about $2.6 \times 10^5 = N_i$. Because this is a 128 pulse average, this is the mean noise power and there is therefore very little fluctuation from bin to bin. The principal features of the signal spectrum are:

---

*The computations were performed by John D. Cremin using orbital elements supplied by William Smith.

†The subscript i is used to index the Doppler bins (filters) where $i = 0, \pm 1, \pm 2, ---, \pm 50$.

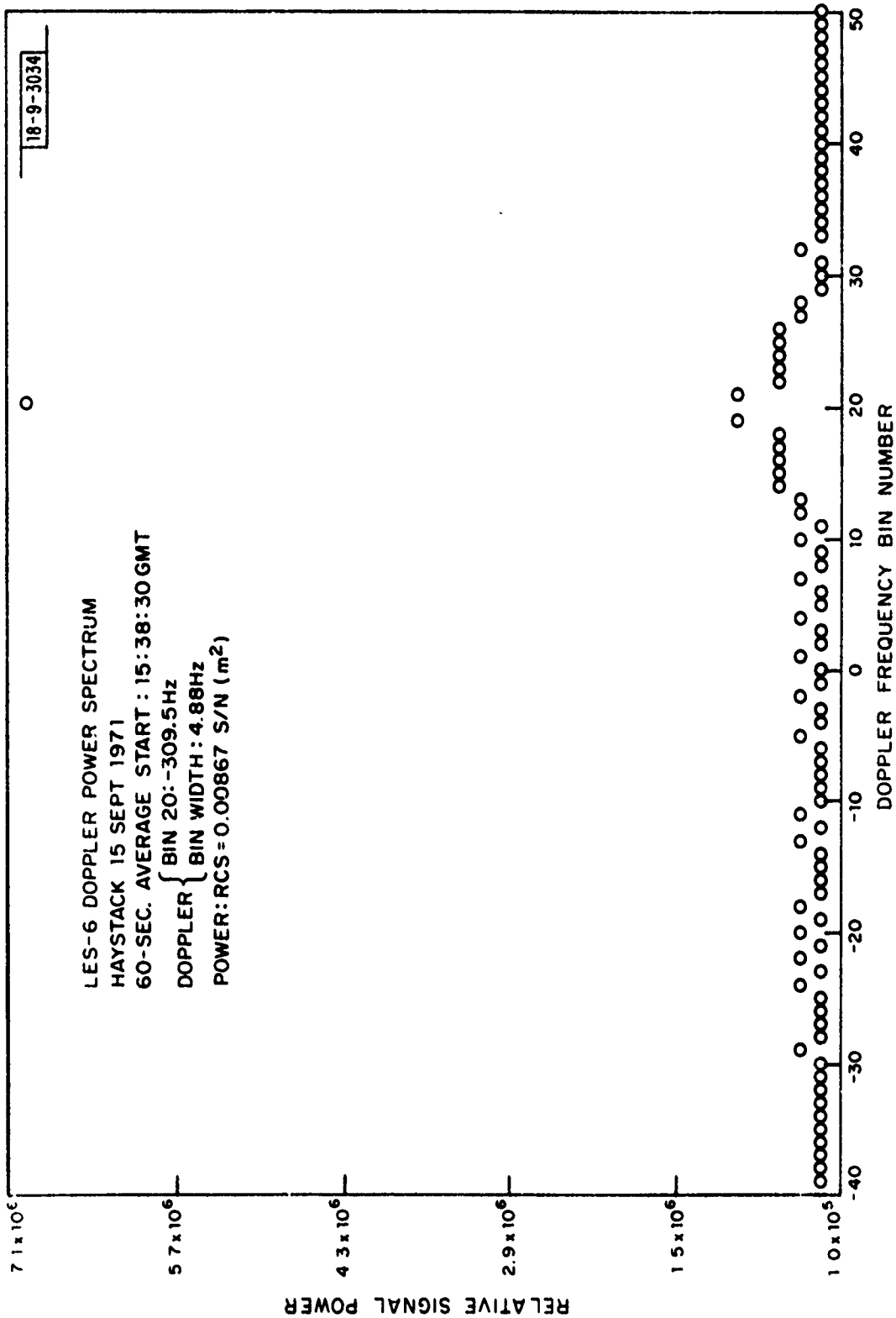

Fig. 9. Doppler spectrum of LES-6.

1. A single narrow peak (width < 4.88 Hz) at $i = +20$, whose value of $S_i + N_i \simeq 70 \times 10^5$.
2. A symmetric pedestal under this peak whose magnitude appears constant at $S_i + N_i \simeq 6.25 \times 10^5$ and whose width is $15 \pm .5$ bins or 73 Hz.

From this spectrum we can deduce the following information about LES-6:

1. The magnitude of the average backscattering cross section (RCS) of the central spike component, and of the pedestal component.
2. The product of the spin rate (ω) and the radius corresponding to the maximum observed Doppler spread.

The RCS may be determined, knowing the Haystack radar parameters, by referring to the level of observed noise, assuming that the noise power observed is entirely that which is expected from receiver noise in a 4.88-Hz bandwidth B. Thus the relative level $N_i = 2.60 \times 10^5$ (in Figure 9) is assumed to represent $k T_e B$, where for $T_e = 75^{\circ}K$ and $B = 4.88$ Hz, $k T_e B = -203.12$ dB relative to a watt second. For reference then we note that a value of RCS = σ_{ref} which would yield a signal power equal to noise power would satisfy the equation

$$\frac{S}{N} = 1 = \frac{P G_t A_r \sigma_{ref}}{(4\pi)^2 R^4 k T_e B} \quad .$$

For the Haystack radar

P = transmitter power during the pulse = 50 dBw

G_t = antenna gain on transmit = 66 dB

A_r = effective antenna receiving area = 26.7 dBm^2

R^4 = (radar range to the satellite)^4 = 303.5 dBm^4.

For these values $\sigma_{ref} = -20.62$ dBm^2.

Using this reference and the relative power levels observed on Figure 9, i.e.,

$$S_i(\text{peak}) + S_i(\text{pedestal}) + N_i = 69.25$$
$$S_i(\text{pedestal}) + N_i = 6.25$$
$$N_i = 2.60,$$

we find that

$$\frac{S_i(\text{peak})}{N_i} = \frac{69.25 - 6.25}{2.60} = 24.23 \text{ or } 13.84 \text{ dB}$$

and

$$\frac{S_i(\text{pedestal})}{N_i} = \frac{6.25 - 2.63}{2.60} = 1.404 \text{ or } 1.47 \text{ dB}$$

from which the estimated values of $\sigma(\text{peak})$ and $\sigma_i(\text{pedestal})$ are

$$\sigma(\text{peak}) = 0.21 \text{ m}^2, \text{ or } -6.78 \text{ dBsm}$$
$$\sigma_i(\text{pedestal}) = .0122 \text{ m}^2, \text{ or } -19.15 \text{ dBsm}.$$

It is also interesting to note that the total cross section represented in the pedestal, i.e., 15 σ_i(pedestal) is equal to $15 \times .0122 \text{ m}^2 = .183 \text{ m}^2$ or - 7.39 dBsm, which is nearly the same cross section as indicated for the central spike. Thus if one were interested in the total RCS unresolved by Doppler frequency, it would correspond to the sum of the two components which, for the example of Figure 9 is 0.39 m^2 or - 4 dBsm.

The cross sections are tabulated in Table I for the observation times and positions plotted in Figure 7. The actual value of the Doppler frequency corresponding to the central spike may be read for the corresponding positions from Figure 8. We will return to the implications of the cross sections shown in the table, which incidentally are reasonably reproducible over these observations and show no consistent trend.

TABLE I

Average (60 sec) radar cross sections of LES-6 from Haystack runs on 15 September 1971. σ(peak): central spike < 4.88 Hz Doppler frequency width; σ_i(pedestal): cross section per 4.88 Hz bin of pedestal 73 Hz wide; $\Sigma_i(\sigma_i)$: total cross section.

Start Run GMT	Elevation Angle (degrees)	σ(peak) (meters)^2	σ_i(ped) (meters)^2	Σ_i (meters)^2
14:46:20	29.831	0.204	0.012	0.380
14:57:00	29.780	0.188	0.008	0.310
15:15:00	29.707	0.216	0.009	0.348
15:38:30	29.585	0.212	0.009	0.348
15:59:10	29.495	0.223	0.010	0.366
16:13:00	29.428	0.242	0.010	0.390
16:33:00	29.344	0.209	0.009	0.349
16:48:00	29.282	0.195	0.009	0.329
17:02:00	29.218	0.225	0.011	0.387
	Average	0.213	0.010	0.356

First, however, let us consider the kind of scattering feature that could contribute to the pedestal component of RCS. Our experience with planetary radar measurements suggests that the spin of the satellite is the source of the Doppler spread. However, a uniformly illuminated, perfectly conducting cylinder, rotating about its axis, will not generate a Doppler spread. We are thus led to look for isolated scatterers on the satellite and the dipole-plus-slot radiators immediately suggest themselves. There remain three questions to be answered:

1. Why is the pedestal flat topped?
2. Is the magnitude of the Doppler spread in agreement with this model?
3. Is the observed RCS reasonable?

In order to produce a flat Doppler spectrum, analysis shows that the RCS of the discrete scatterers must vary as $\cos\phi$, where ϕ is the rotation angle measured from the direction to the radar, i.e., as the projected area of a surface element, zero at the limb and maximum at the center. If we were dealing simply with dipoles standing well off the cylindrical surface, this result would be disturbing. Since we are in fact dealing with a scatterer that consists of a dipole, a slot, and a section of (cylindrical) ground plane, it is less surprising. However, we have not attempted to analyze these antenna elements theoretically, nor have we measured a model.

The rotation rate of the satellite is well known from telemetry and the value can be verified from long-term recordings of the amplitude of the radar return versus time (a short interval is shown in Figure 3). The radar data indicate a period of $6.66 \pm .03$ seconds, or $\omega = 0.943$ radians/sec. To account for the observed maximum relative Doppler frequency spread of 36.5 Hz halfwidth, the scatterers must be at a radius r given by

$$r = \frac{c}{2f} \frac{f_D}{\omega} = 74.1 \text{ cm} \quad .$$

Since the slots are at a radius of 61 cm and the dipoles are at a radius of 76 cm, a value of 74 cm for the combined scattering center is quite satisfactory.

Finally, we make a crude estimate of the radar cross section of a low-frequency dipole. The dipoles are 51 cm long, so that the resonant wavelength λ_o is about 85 cm ($l = 0.6\ \lambda_o$). Since the dipoles are not viewed in their broadside (main) lobe, we use the spatial and polarization average value for the RCS which is $0.27\ \lambda_o^2$. For shorter wavelengths, we assume that the RCS will vary as λ. Hence at the radar frequency

$$\text{RCS} = 0.27 \times (.85\ \text{m})^2 \times \frac{.038}{.85} = .0087\ \text{m}^2$$

$$= -20.6\ \text{dBsm} \quad .$$

This is close to the average RCS per Doppler bin, which is reasonable since only one dipole contributes to a bin at a time. Considering the crudeness of the approximation and the neglect of the slot and ground plane, the agreement is very good. Thus we have accounted for all the characteristics of the Doppler pedestal.

What now accounts for the central spike, if the dipoles account for the pedestal? As suggested in the discussion of the Doppler pedestal model, a smooth, perfectly conducting cylinder would give just such a narrow spike and we have not as yet accounted for scattering by the main body of LES-6. In particular, let us consider the scattering from the sidelobes of an ideal cylinder whose axis precesses during rotation and which is sampled several times per rotation. Figure 10 is a plot of the sidelobe pattern of an idealized conducting cylinder of the same dimensions as LES-6 when viewed at the Haystack radar frequency ($\lambda = 0.0382$ m). We can see that the lobe separation is about 0.65 degrees and the RCS at the lobe peaks ranges from about $0.32\ \text{m}^2$ to about $0.12\ \text{m}^2$ for the range of aspect angles θ applicable. Suppose the cylinder were stationary and viewed at some aspect angle θ_o, then one would see a single value of RCS corresponding to θ_o. If the ideal cylinder were rotating about its symmetry axis with angular velocity ω, RCS would still have this single value. However, if the cylinder were tilted at an

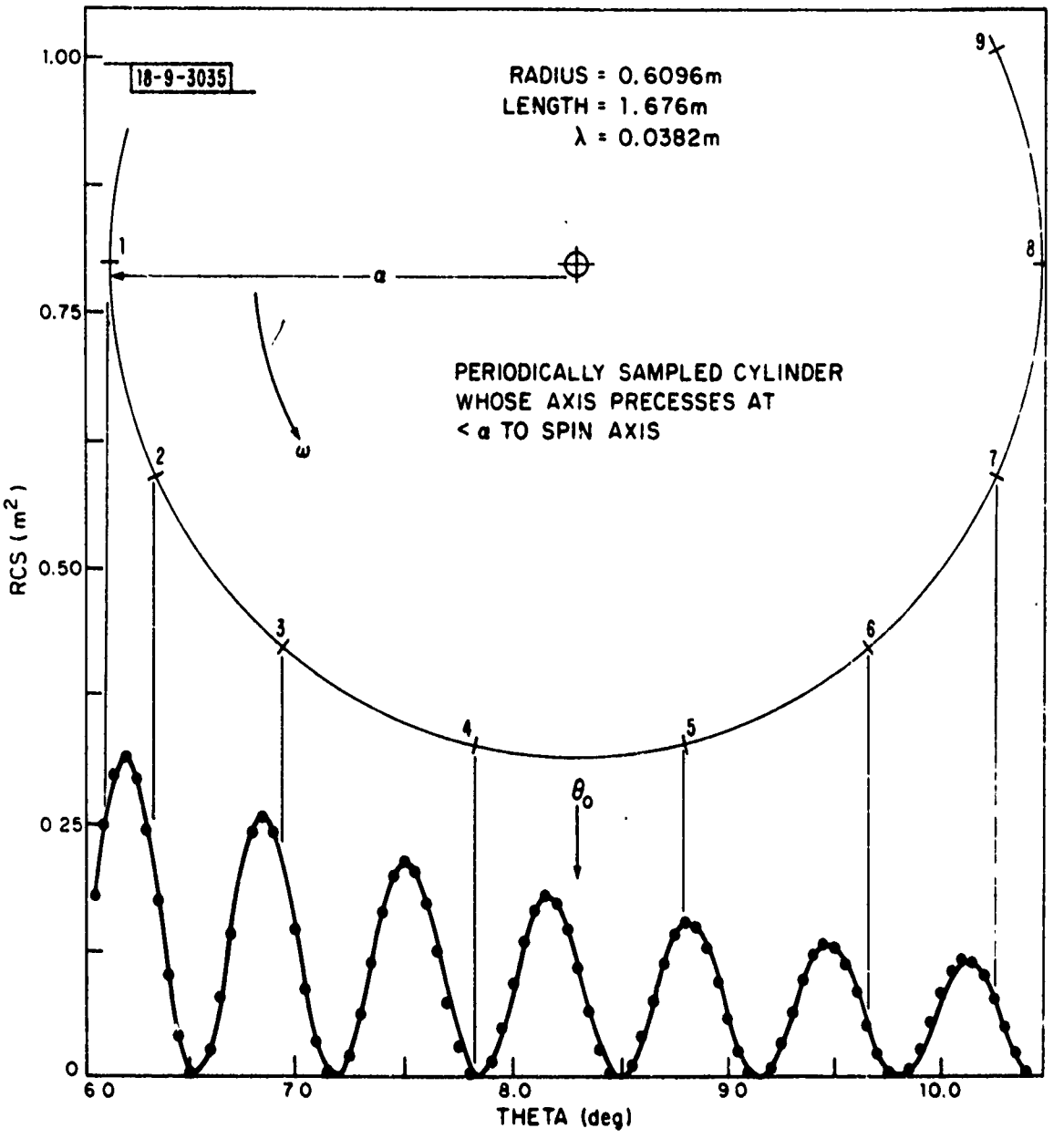

Fig. 10. RCS of conducting cylinder vs aspect angle.

angle α with respect to the angular velocity vector, then the aspect angle θ would be a function of time

$$\theta = \theta_0 + \alpha \cos(\omega t + \beta)$$

where β is just the initial phase angle at zero time. The RCS at any instant would depend on the value of θ.

Efforts to produce a pattern like that of Figure 3 with this model failed. There are about 14.18 samples per rotation of the satellite and there are usually two large peaks separated by two or three small peaks. Furthermore, peaks as high as 2.67 m^2 are observed, almost ten times the RCS suggested by the simple model.

A more elaborate model (EHECY) was tried consisting of three major contributors:

- one pair of electric dipoles, each of length L_1, in line, and separated on centers by a distance S.
- one pair of magnetic dipoles, each of length L_1, in line, separated on centers by a distance S, and displaced a distance D behind the electric dipoles.
- one ideally conducting cylinder of length L_2 and radius R, whose axis is parallel to and in the plane of the two pairs of dipoles, and whose surface contains the magnetic dipoles (slots).

The plane of symmetry for all three elements is the same and is perpendicular to the cylinder axis. For small values of α, θ is very nearly the same as the aspect angle. The angle ϕ represents rotation of the dipoles about the cylinder axis, measured from the plane containing the line-of-sight and the cylinder axis. Dipoles close to the limb are not included in the model because they will show a Doppler shift and will not contribute to the spike at zero relative Doppler.

Figure 11 is a plot of the sidelobe pattern for $\phi = 0$ and $1.5^\circ < \theta < 10^\circ$. Note the strong peak at $\theta = 7.5^\circ$. Figure 12 is a pattern taken in the other plane: $\theta = 7.5^\circ$ and $0 < \phi < 20^\circ$.

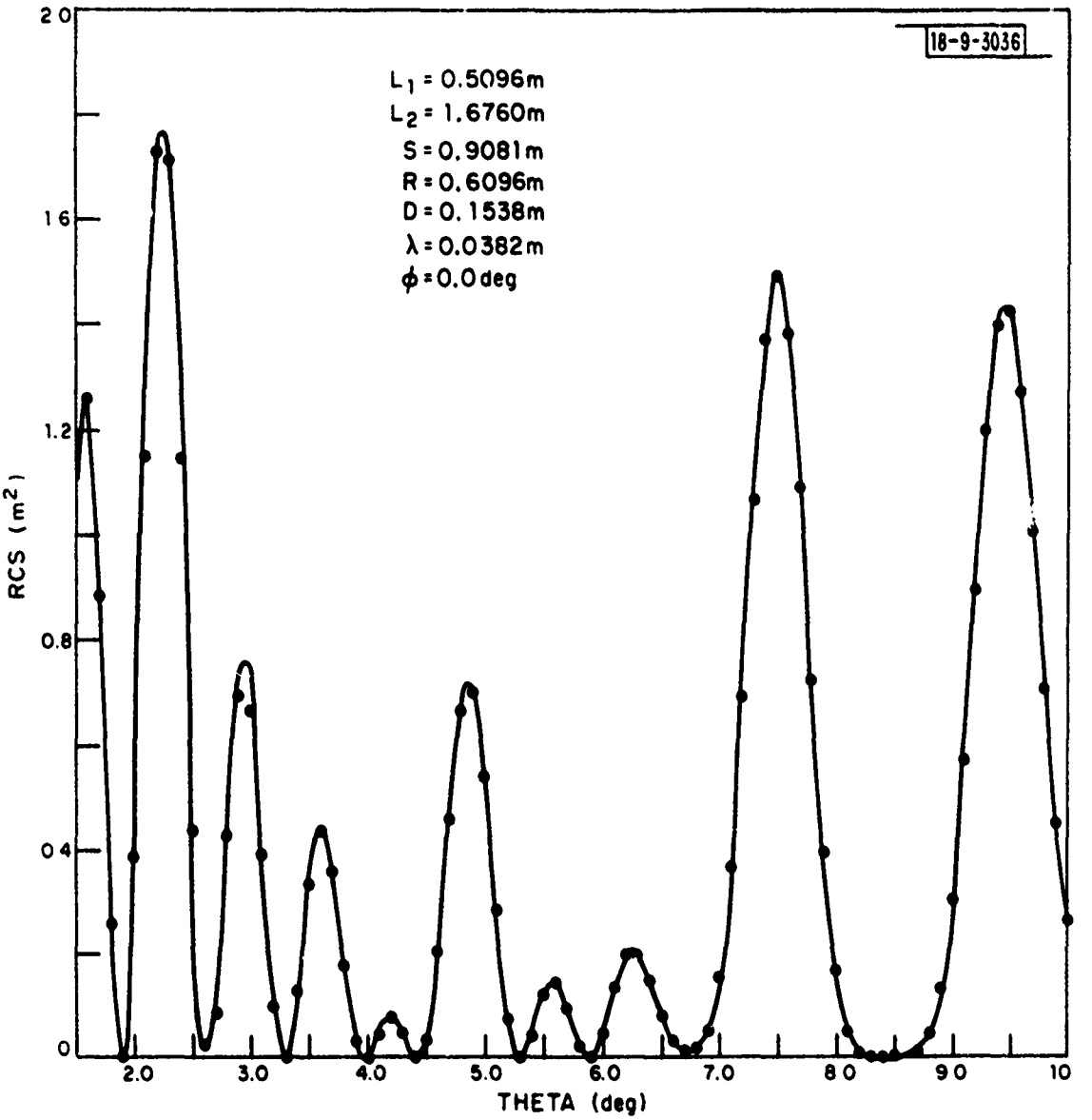

Fig. 11. EHECY model for σ plotted for variation in tilt angle, $\theta(1.5 \rightarrow 10^{o})$.

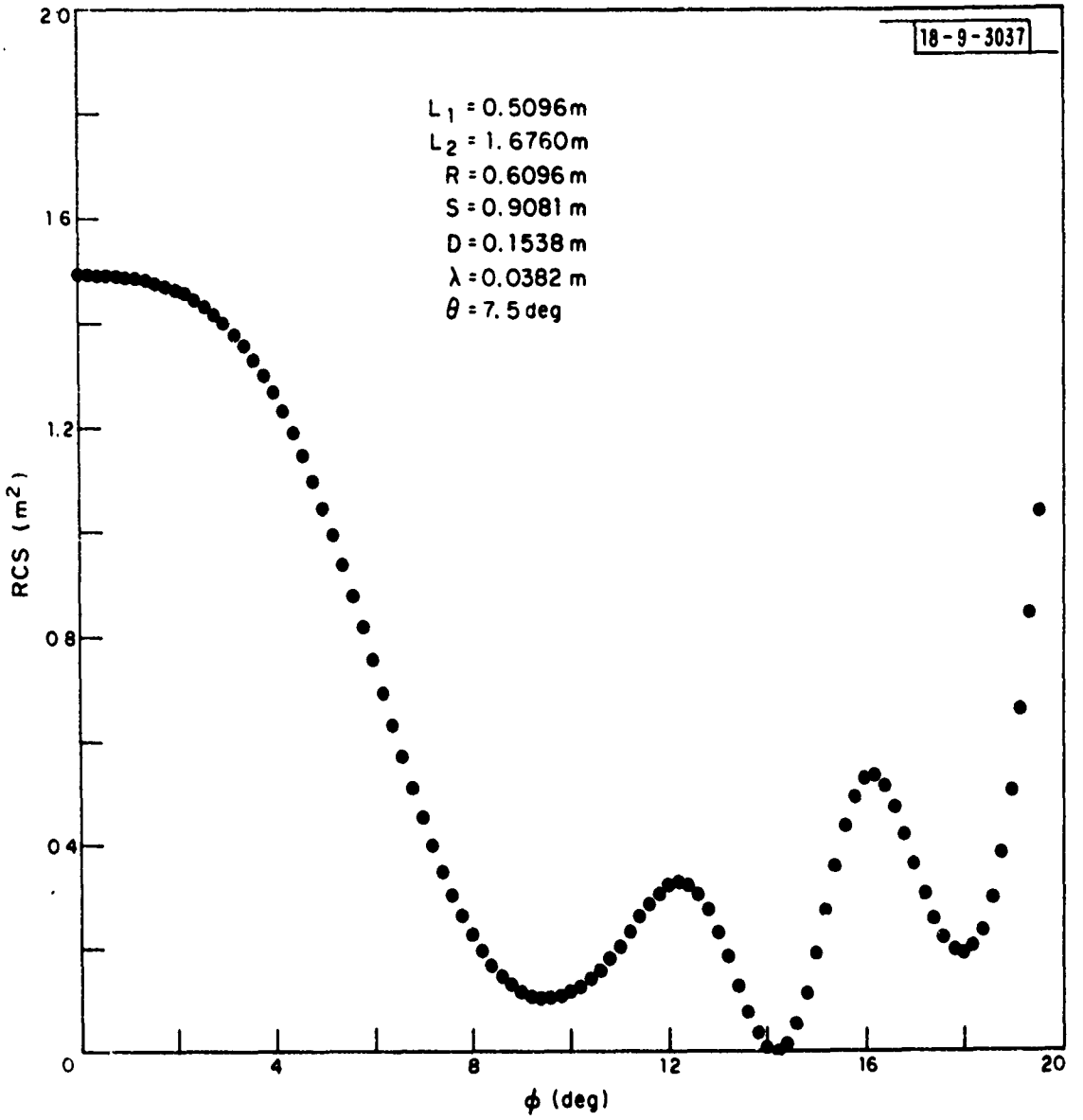

Fig. 12. EHECY model for cross section σ plotted for variation in rotation angle, θ ($0 \rightarrow 20^{o}$).

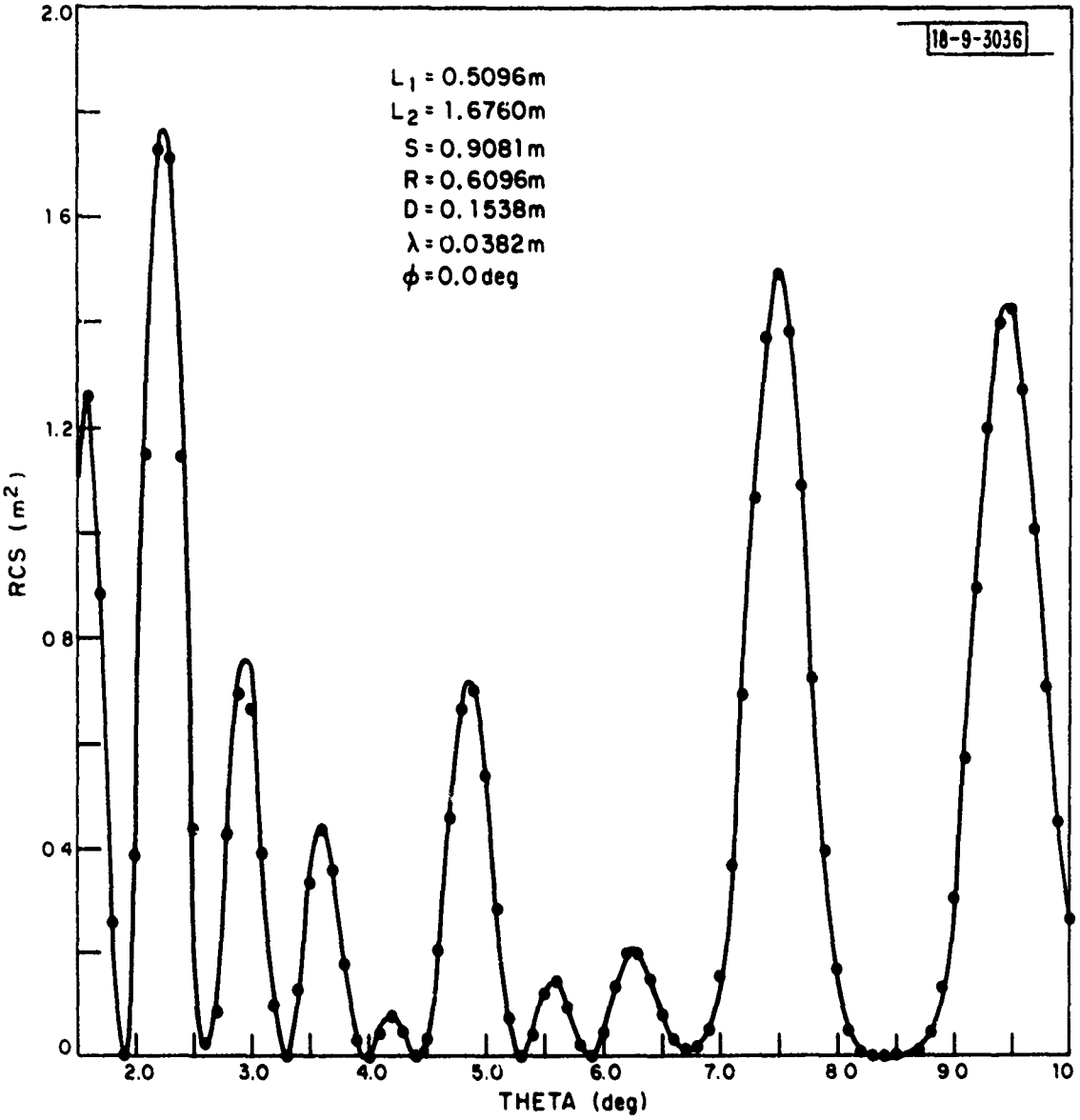

Fig. 11. EHECY model for σ plotted for variation in tilt angle, $\theta(1.5 \rightarrow 10^{o})$.

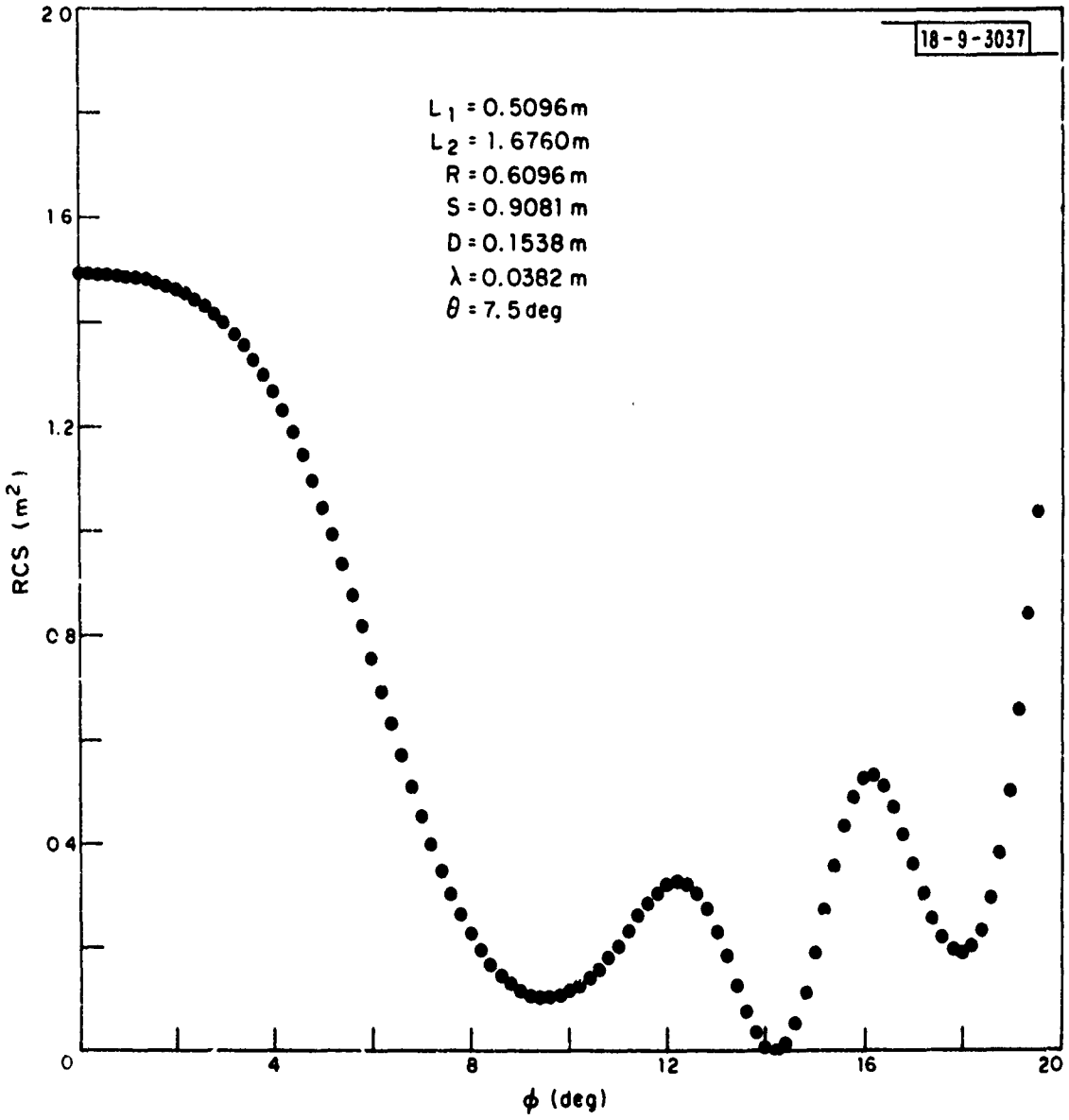

Fig. 12. EHECY model for cross section σ plotted for variation in rotation angle, θ (0 → 20°).

Clearly the lobe width and amplitude decrease as ϕ departs from zero. Even though the RCS occasionally reaches the same peak value for $\phi \neq 0$, the value averaged over a sample width (0.2-second radar pulse), which is about 11° of rotation, will be significantly less than near $\phi = 0$. This accounts for the narrowness of the zero-Doppler spike.

From Figure 11 one can see the origin of the type of pulse-by-pulse return sequence observed in Figure 3. The pair of dominant returns separated by three and nine lower returns alternately are precisely what would be observed by periodic sampling, with θ varying cyclically by rotation as suggested earlier. With $\theta_o = 6.3^{\circ}$, the pair of peaks would correspond to two samples near 7.5°.

Table II shows two detailed calculations. Note that the actual sampling rate is about 14.18 samples per revolution rather than an integral number, so that the observed return will slowly slide along as if β were constantly changing. Note also that ϕ never exceeds $\pm 22\ 1/2^{\circ}$ because outside those limits a different set of dipoles comes into play (there are eight sets of dipoles around the satellite).

Thus the EHECY model appears capable of explaining the important features of the pulse-by-pulse radar return.

Finally, in Table III we summarize the principal observed characteristics and compare them with values computed from the EHECY model.

CBS:GLG:kaf

TABLE II

Computed radar cross sections for the EHECY model with the following parameters: $L_1 = .5096$, $L_2 = 1.676$, $S = .9081$, $R = .6096$, $D = 1538$, $\lambda = .0382$ all in meters, $\theta_o = 6.30^o$, $\alpha = 2.2^o$. Fourteen samples per rotation. β = starting phase for ϕ.

	$\beta = 0$				$\beta = -6.43^o$			
Sample	θ	ϕ	f_D	RCS	θ	ϕ	f_D	RCS
0, 14	4.10^o	0^o	0 Hz	.047 m^2	4.11^o	-6.43^o	- 3.9 Hz	.040 m^2
1, 13	4.32	19.28	11.5	.012	4.22	12.86	7.5	.184
2, 12	4.93	- 6.43	3.9	.158	4.74	-12.86	- 7.5	.300
3, 11	5.81	12.86	7.5	.018	5.57	6.43	3.9	.000
4, 10	6.79	-12.86	- 7.5	.003	6.55	-19.28	-11.5	.069
5, 9	7.67	6.43	3.9	.580	7.47	0	0	1.482
6, 8	8.28	-19.29	-11.5	.075	8.16	19.28	11.5	.193
7	8.50	0	0	.001	8.49	- 6.43	- 3.9	.001

TABLE III

SUMMARY OF OBSERVATIONS AND CALCULATIONS FROM THE EHECY MODEL

	Observed	Calculated
Average pedestal height	.012 m^2 (Fig. 9) .010 (Table I)	.022 m^2
Average zero-Doppler (Spike)	.21 m^2 (Fig. 9) .213 (Table I)	.252 m^2
Largest RCS	2.67 m^2 (Fig. 3)	1.48 m^2

First order patterns of pulse-by-pulse total cross section agree with the sequence: 9(10) low, 1 high, 3(2) low, 1 high, repeat.

Maximum radius estimated from radar data is 0.74 m. Actual dipoles are at a radius of 0.76 m.

REFERENCES

1. H. G. Weiss, "The Haystack Microwave Research Facility," IEEE Spectrum, (February 1965), pp 50-69.

2. D. C. MacLellan, H. A. MacDonald, P. Waldron, and H. Sherman, "Lincoln Experimental Satellites 5 and 6," AIAA 3rd Communications Satellite Systems Conference, (April 1970). (AIAA Paper No. 70-494, NASA Cat. 3431)